INVESTIGATION OF ROTATION SYMMETRIC FLOWS WITH CONSTANT SPIN

By

F. BENCZE, L. MOLNÁR and G. DEMETER

Department of Fluid Mechanics, Technical University, Budapest

(Received October 3, 1968)

Presented by Prof. Dr. J. GRUBER

STRSCHELETZKY [1] studied the theory of the hydrodynamic equilibrium of flows with spin. According to his theory, an incompressible fluid assumed to be frictionless, flowing in a straight pipe of circular cross-section and carrying out forward and rotary movement simultaneously, will produce a cylindrical parting surface in the pipe, outside of which the fluid performs a rotary movement according to its spin and a forward movement in accordance with the criteria of continuity. This range of flow will be hereinafter referred to as the "sound flow". Within the parting surface the axial velocity will be zero and the fluid will rotate like a solid body. The range of the fluid flow in rotary movement will hereinafter be termed "eddy core".

Applying the Euler-Moupertuis principle, Prof. STRSCHELETZKY states that fluid cannot flow unless it is in a hydrodynamic equilibrium, viz. the time integral of the kinetic energy of the medium — the so-called effect integral — is at a minimum. From this fact it follows that the modification of the characteristics which determine the state of equilibrium (for instance, the radius of the parting surface), by a differential value, the value of the effect integral remains unchanged.

Assuming stationary flow and that at a certain distance from the entry, the distribution of velocity and pressure in the pipe measured in the meridional section becomes constant, the flow characteristics in this problem are independent of the time t and the coordinate z.

Assuming furthermore that the said parting surface may actually form, let us write the effect integral of the flow in two steps.

a) The effect integral for a fluid ring extending from the parting surface to the pipe wall, of a length Δl, can be written in the following form:

$$I_k = \int_{t_1}^{t_2}\int_0^{2\pi}\int_{r_i}^{R} \varrho(r\, d\varphi\, dr\, \Delta l)\,\frac{c^2}{2}\, dt \tag{1}$$

According to our assumption, there is a complete symmetry in the meridional section and the flow parameters are independent of φ. Thus, after integration with respect to φ and t, we obtain:

$$I_k = \pi \varrho \, \Delta l \, (t_2 - t_1) \int_{r_i}^{R} c^2 \, r \, dr \tag{2}$$

The resultant velocity c of the medium in flow consists of two components, the meridional velocity c_u and the axial velocity c_a.

Assuming constant spin Γ of the flow medium along the radius, the distribution of the meridional velocity along the radius is determined by:

$$c_u = \frac{\Gamma}{2\pi r} \tag{3}$$

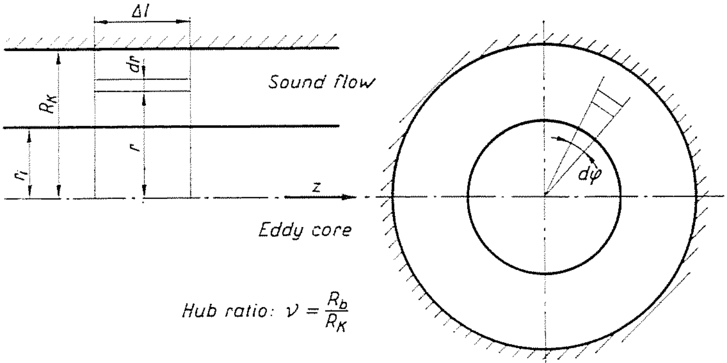

Fig. 1. Sketch of the location of the eddy core

The axial velocity can be calculated according to the formula:

$$c_a = \frac{Q}{\pi(R^2 - r_i^2)} \tag{4}$$

The resultant velocity is obtained from the components:

$$c = \sqrt{\frac{\Gamma^2}{4\pi^2 r^2} + \frac{Q^2}{\pi^2 (R^2 - r_i^2)^2}} \tag{5}$$

From the volume of the cylinder of length Δl, the value of Δl can be expressed as:

$$\Delta l = \frac{\Delta V}{\pi(R^2 - r_i^2)} \tag{6}$$

Introducing the relations (5) and (6) into Eq. 2, we obtain

$$I_k = \frac{\varrho \Delta V (t_2 - t_1)}{\pi^2 (R^2 - r_i^2)} \int_{r_i}^{R} \left[\frac{\Gamma^2}{4r^2} + \frac{Q^2}{(R^2 - r_i^2)^2} \right] r dr$$

After integration:

$$I_k = \frac{\varrho \Delta V (t_2 - t_1)}{2\pi^2 (R^2 - r_i^2)} \left[\frac{\Gamma^2}{2} \ln \frac{R}{r_i} + \frac{Q^2}{R^2 - r_i^2} \right] \tag{7}$$

b) The effect integral for the eddy core can be written in a similar way:

$$I_b = \int_{t_1}^{t_2} \int_0^{2\pi} \int_0^{r_i} \varrho (r d\varphi \, dr \, \Delta l) \frac{c^2}{2} dt$$

Integration with respect to t and φ:

$$I_b = \pi \varrho \Delta l \, (t_2 - t_1) \int_0^{r_i} c^2 r \, dr$$

The spin ($\Gamma = 2\pi r_i c_{u_i}$) on the parting surface determines a meridional velocity (c_{u_i}) from which the angular velocity of the eddy core can be calculated:

$$\omega = \frac{c_{ui}}{r_i}$$

whence

$$c_u = r \frac{c_{ui}}{r_i}$$

Substituting the c_{u_i} value obtained from the spin, we arrive at the following correlation:

$$c_u = r \frac{\Gamma}{2\pi r_i^2}$$

However, in the eddy core the velocity c is equal to c_u. Accordingly, the effect integral will be

$$I_b = \frac{\varrho \Delta l \, (t_2 - t_1) \, \Gamma^2}{4\pi \, r_i^4} \int_0^{r_i} r^3 \, dr$$

Integration yields:

$$I_b = \frac{\varrho \Delta l \, (t_2 - t_1) \, \Gamma^2}{16 \, \pi} \tag{8}$$

The effect integral relating to the entire flow will be equal to the sum of the effect integrals of the two flow ranges:

$$I = I_k + I_b$$

Now, that r_i value for which the effect integral is at its minimum, must be determined. This condition can be determined from the relation

$$\frac{dI}{dr_i} = 0$$

Since however, I_b is independent from r_i, $\frac{dI_b}{dr_i}$ is a priori equal to zero and the equation

$$\frac{dI_k}{dr_i} = 0$$

determines the resolution of the problem.

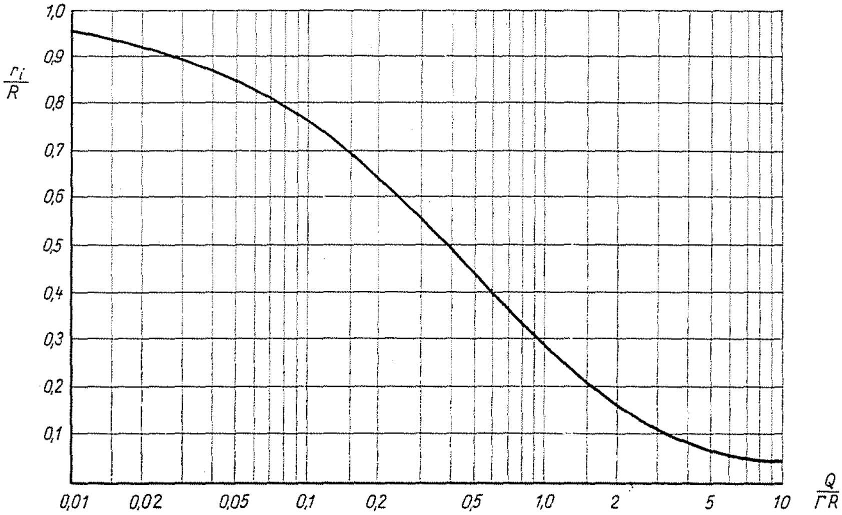

Fig. 2. Variation of the relative eddy core radius as a function of $\frac{Q}{\Gamma R}$

According to what went before, we have obtained the following result:

$$\frac{Q}{\Gamma R} = \frac{1}{2}\sqrt{\frac{1}{2}\left(\frac{R}{r_i}\right)^2\left[1-\left(\frac{r_i}{R}\right)^2\right] - \ln\frac{R}{r_i}\left[1-\left(\frac{r_i}{R}\right)^2\right]} \tag{9}$$

Fig. 2 shows the variations of $\frac{Q}{\Gamma R}$ as a function of $\frac{r_i}{R}$ on the basis of relationship.

Rendering the values dimensionless, the experimental results obtained by two different methods can be compared.

By the analysis of the second differential quotient of the effect integral, it can be proved that the function actually has a minimum at the point under study.

However, the idea may arise that more than one parting surfaces would evolve in the pipe. It might be assumed that another parting surface would develop between the pipe wall and the sound flow and cause an eddy ring, similar to the eddy core, to form between the pipe wall and medium, respectively, that an arbitrary number of eddy rings would evolve in the pipe.

To prove that no eddy rings can come about apart from the eddy core, we may write down the effect integrals for the assumed cases. Their sum

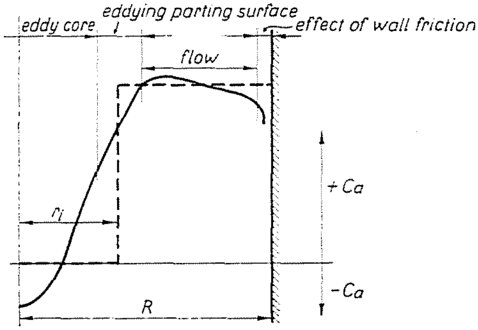

Fig. 3. Distribution of axial velocity with friction

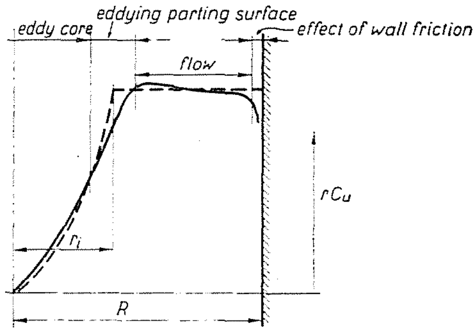

Fig. 4. Distribution of spin with friction

will be found to exceed the value of the effect integrals written above and according to the Euler-Moupertuis principle, no more parting surface or eddy rings can form.

The velocity distribution prevailing in the flow of ideal, frictionless medium described by STRSCHELETZKY, will change in frictional cases, as illustrated in Figs 3 and 4.

With a frictional medium, in place of the theoretical parting surface, an eddy layer of increasing thickness will evolve as indicated in Fig. 5.

Experience has shown that in direction z, i.e. along the pipe axis, flow becomes constant at a distance 3 D from the device causing the spin.

As a result of friction, there will be no sharp transition between the velocity of the eddy core and that of the sound flow.

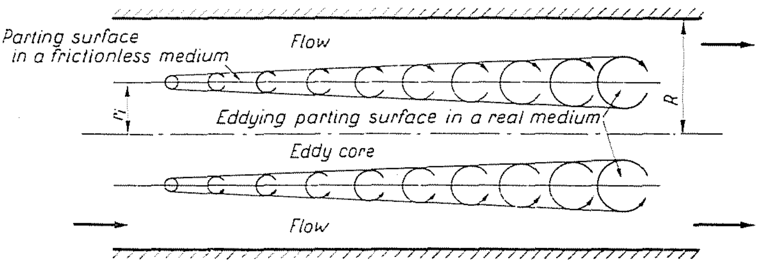

Fig. 5. Eddying layer in frictional media

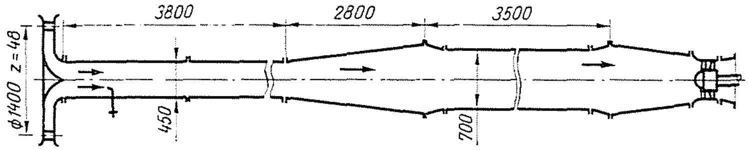

Fig. 6. Schlünkes' test setup with radial cascade

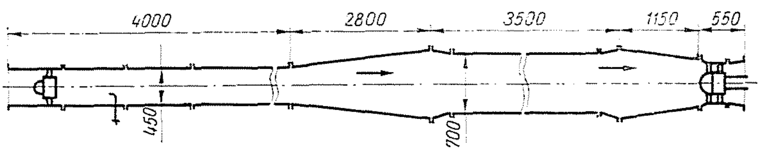

Fig. 7. Schlünkes' test setup with axial cascade

1. Experimental results

Schlünkes [1] verified the theory of rotation symmetric flow with constant spin by experiments. In a series of systematic experiments he examined the behaviour of two media, air and water, with respect to the formation of eddy core. Schlünkes' experimental setup consisted of a guide cascade, an adjoining cylindrical measuring pipe, and an axial fan (Figs 6 and 7).

Axial and radial blades were used for the cascades. However, the radial cascade proved unreliable in test, it being unfit to ensure a stationary state and produced an asymmetric oscillating eddy about the pipe axis.

Although the experiments with axial blades confirmed an eddy core to exist, its radius as measured by Schlünkes was always slightly smaller than the calculated value.

Schlünkes found axial guide vanes likely to produce a flow closely approximating the theoretical one, since these produce spin at the given radius and permit adherence to the calculated values.

The central part of the axial cascade is a hub; partly because at this point the high degree of deflection for a constant spin cannot be achieved anyway and partly to serve for fixing the blades.

The hub in SCHLÜNKES' experiments terminated at a short distance behind the plane of the cascade.

The idea was propounded that the fundamental factor causing the parting surface to evolve, was the separation behind the hub, while the flow behind the separation became regularized according to the above outlined laws.

It was therefore necessary to carry out experiments in which there existed no factor to cause separation.

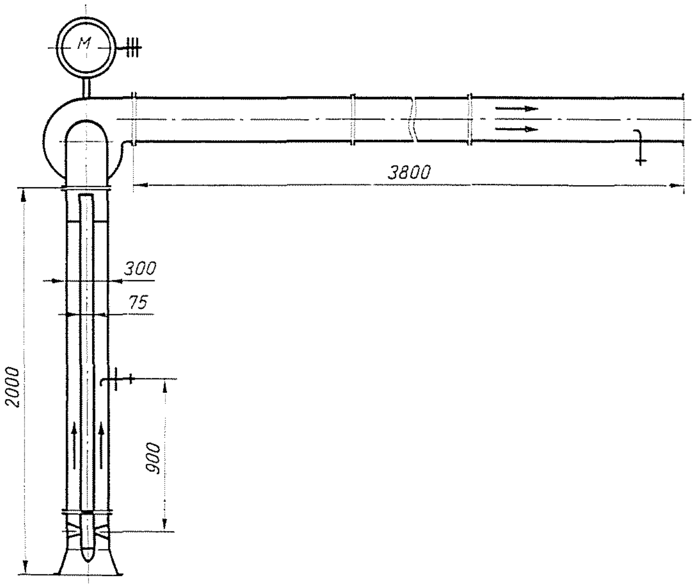

Fig. 8. Schematic layout of the setup in tests

Our test rig differed from the one used by SCHLÜNKES in that the hub of the device producing spin extended along the full length of the pipe. The hub radius had of course to be smaller than that of the parting surface calculated from the parameters of the test rig.

Fig. 8 shows the schematic layout of the test rig. Spin was produced by a conventionally dimensioned arched cascade. Since experience showed the final flow pattern to evolve at a distance 3 D, the gauges were located accordingly.

The pipe acting as hub extending along the full length of the rig, was suspended by steel wires. This method of fixing caused a minimum of flow resistance and its impact on the readings was likewise negligible.

SCHLÜNKES determined the flow volume from the velocity pattern evolved in the flow with spin. To be independent of the uncertainties inherent with the determination of average spin flow velocities, the quantity measurements were carried out in the delivery pressure hub, along the standard procedure.

Fig. 8 shows the main dimensions of the structural elements, and the location of the measuring points.

Lacking a suitable gauge for the rather complicated job, we used a four-tube velocity-direction probe of our own design, calibrated at the laboratory of the Department of Fluid Mechanics of the Technical University, Budapest.

In spite of the fact that in the flow of a real medium a thick eddying layer is forming, instead of the theoretically determined parting surface,

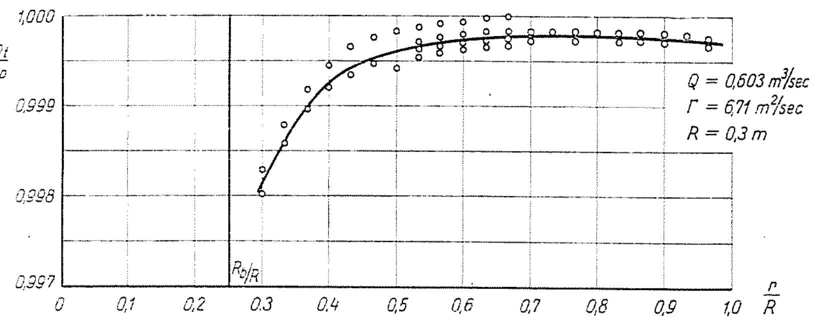

Fig. 9. Distribution of the total pressure

the charts compiling test findings unambiguously indicate the evolution of an eddy core in accordance with the theoretical assumption.

Let us examine now the findings of our experiments and see what conclusions can be drawn concerning the determination of the radius r_i.

a) Fig. 9 shows the curve $\dfrac{p_t}{p_0} = f\left(\dfrac{r}{R}\right)$. It is obvious that, assuming frictionless flow, the total pressure in the range of sound flow will be constant but it will parabolically decrease in the eddy core and so, the theoretical curve will show a break at the parting surface.

In actual flow the friction arising in the eddy ring near the boundary layer causes a drop in the total pressure. As a result, instead of a sudden drop of the total pressure at the parting surface radius, a gradual transition will arise, according to the function $\dfrac{p_t}{p_0} = f\left(\dfrac{r}{R}\right)$

b) The safest to determine the location of the parting surface is the curve $\left(\dfrac{c_u}{c_{a\,\mathrm{theor}}}\right) = f\left(\dfrac{r}{R}\right)$ (Fig. 10).

According to the laws of ideal flow, c_u starting from zero in the eddy core, will increase linearly to its maximum at the r_i then hyperbolically decrease in the region of sound flow.

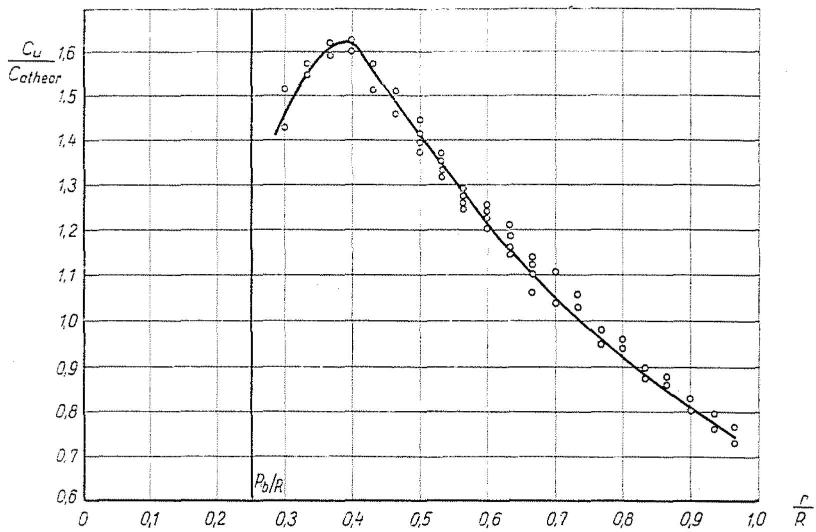

Fig. 10. Distribution of meridional velocity

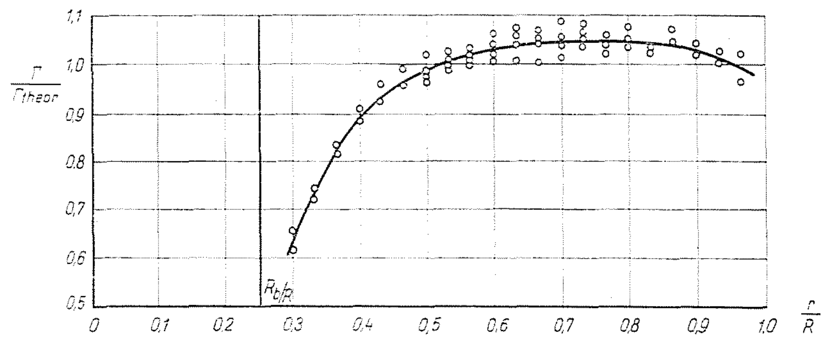

Fig. 11. Distribution of spin

Also the function $\left(\frac{c_u}{c_{a\,\text{theor}}}\right) = f\left(\frac{r}{R}\right)$ determined by measurements under real conditions shows similar properties. The maximum of $\left(\frac{c_u}{c_{a\,\text{theor}}}\right)$ is at $\frac{r}{R} = 0.39$.

c) Fig. 11 illustrates the ratio of the measured to the projected spin as a function of the ratio between the stationary $(r_2)T$ and the moving radii. While in sound flow the value of $\frac{\Gamma}{\Gamma_{\text{theor}}}$ corresponding to constant spin remains unchanged in the eddy core it shows a parabolic regression due to its rotation as a solid body. The result shows that outside the eddy core and excepted the layer immediately at the wall, a constant spin was maintained.

d) If a frictional medium is made to flow—and even more particularly in case of vigorous mixing—it is inconceivable that axial velocity at the parting surface should suddenly drop to zero. It may by expected—and this was confirmed by our measurements (Fig. 12) — that velocity decreases gradually, over a wide range. Nevertheless, this curve did not permit to draw numerical conclusions.

Along the external wall, the effect of wall friction is manifest in each curve, and it is possible to determine the thickness of the layer disturbed by friction. Assuming a disturbed layer of similar thickness also near the hub, it did not affect the determination of the radius of the parting surface.

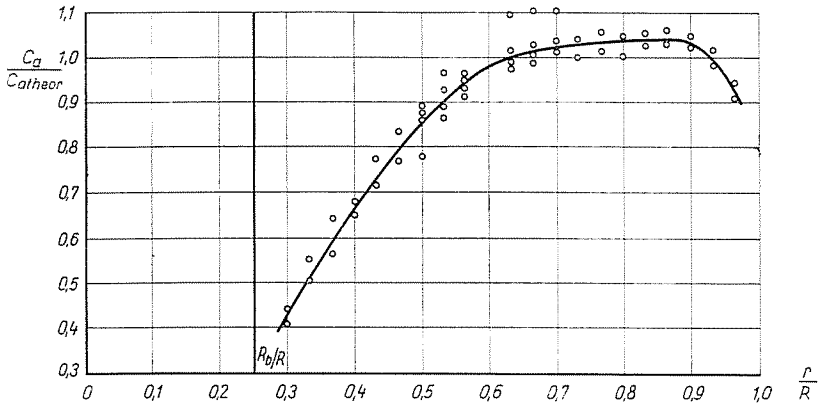

Fig. 12. Distribution of axial velocity

On the basis of the measurement results we may conclude that in the case of flow with spin, a parting surface exists, or better, in case of a frictional medium, the boundary surface transforms into a parting surface, in conformity with real circumstances.

On ground of the examination of the flow characteristics in radial direction, it may finally be stated that in our experimental setup featured by the given parameters (Fig. 9), the radius of the parting surface, $\frac{r_i}{R}$ is 0.39.

The value of $\frac{Q}{\Gamma R}$ was determined in two ways. The first process was the following:

$$\frac{Q}{\Gamma R} = \int_{R_b}^{R} \frac{dQ}{\Gamma R} = \frac{1}{R} \int_{R_b}^{R} \frac{c_a}{c_u}\, dr$$

According to the other process, the individual factors were calculated separately; as a consequence, the value of circulation calculated with the formula

$$\Gamma = 2\pi \int_{R_b}^{R} c_u\, dr$$

and the value of Q measured on the orifice were taken into consideration. Calculations have proved that the value of $\frac{Q}{\Gamma R}$ fairly approximates the theory.

Also the value of $\frac{r_i}{R}$ as derived from the tests and the theoretical one plotted in Fig. 2, respectively, are in good agreement.

From experience we have formed the view that for the further elucidation of the phenomenon, experiments should be performed with the hub rotating at a given circumferential speed, since this would enable to eliminate the effect of the hub friction on the distribution of the velocity c_u along the radius.

2. Restrictions of the hub dimensions in axial fans

The theory outlined in Chapter 1 may have an influence on the dimensioning of the hub of axial-flow machines operating according to the Euler principle.

It may be assumed that the eddy core evolves gradually along the blades causing spin, and may produce losses through disturbing the flow as soon as between the blades.

It is obvious from what went before that in machines with axial flow, eddy currents must be prevented from forming by applying a hub of due size. The radius of a correctly dimensioned hub is equal to, or greater than, the calculated eddy core radius.

Let us see whether the conventional method of dimensioning can reliably prevent the formation of an eddy core.

The conventional method of determining the hub dimensions takes one single point into consideration: to prevent the separation of flow near the hub. Namely, from the velocity triangles drawn for the wheel, it is obvious that, for instance with axial-flow fans and pumps, relative velocity decreases while passing between the blades. On the other hand, a deceleration is known to be permissible up to a certain limit only, without involving the risk of separation. Since — as will be seen later — the rate of deceleration increases toward the hub, the aim of dimensioning is to determine hub dimensions so that no separation arises even in case of a maximum drop of speed at the hub.

Fig. 13 shows the inlet and outlet velocity triangles of the blade of an axial-flow fan on two different radii.

In the design of fans it is customary to assume a constant increase of the total pressure (Δp_t) along the blade. It follows from Euler's equation relating to the axial-flow fan

$$\Delta p_t = \varrho u \Delta c_u$$

that the requirement of constant total pressure along the radius cannot be met unless the velocity component derived from the blade circulation (Δc_u) increases proportionally with the radius decrease.

On hand of the velocity triangles it is obvious that, due to the combined effect of decreasing circumferential velocity and increasing Δc_u for an otherwise identical axial velocity, the rate of relative deceleration will increase in the direction of the hub.

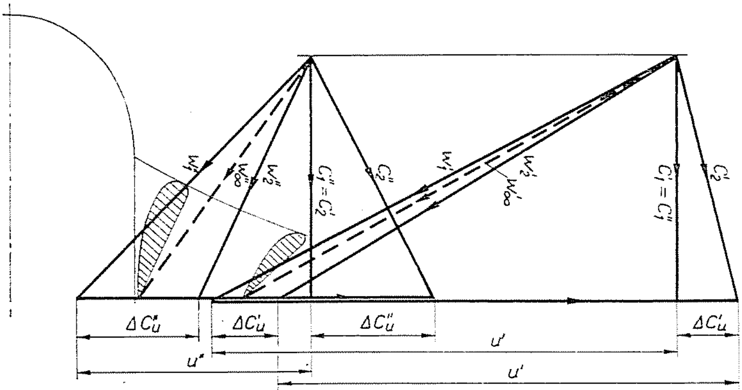

Fig. 13. Variation of the velocity triangles along the blade

In accordance with the conventional dimensioning of axial-flow fans [2], relative deceleration can be confined by limiting the value

$$\left[\frac{l}{t} c_f\right]_{hub} = \frac{2c_a \Delta c_u}{w_\infty^2 \sin(\beta_\infty + \delta)} \tag{10}$$

In fans with a sufficiently large blade pitch $\frac{l}{t} \leqq 0.9$ where thus the effect of cascade is negligible (i.e. the blades of which can be regarded as isolated aerofoils), the upper limit suggested empirically for the value of $\left[\frac{l}{t} c_f\right]_{hub}$, is 0.6 to 0.65.

Making use of the flow coefficient $\varphi = \left(\frac{c_a}{u_k}\right)$ interpreted for axial-flow fans, as well as the pressure coefficient

$$\psi = \frac{\Delta p_t}{\frac{\varrho}{2} u_k^2}$$

and using the value

$$\nu = \frac{R_b}{R}$$

of the hub ratio $\left[\frac{l}{t} c_f\right]_{hub}$ can be calculated in the following manner:

$$\left[\frac{l}{t} c_f\right]_{hub} = \frac{1}{\left[\left(\frac{\varphi}{\psi} \nu\right)^2 - \left(\frac{\nu^3}{\psi} \pm \frac{1}{4}\right)^2\right]^{1/2}} \tag{11}$$

In this relation signs $+$ and $-$ refer to the axial-flow fan with and without prerotation, respectively.

It can be established from Eq. (11) that with a fan characterized by a given φ and ψ, the limit $\left[\frac{l}{t} C_f\right]_{hub} \leqq 0.65$ can be ensured by a suitably chosen hub ratio. To determine this suitable hub ratio, equation (11) is rearranged:

$$\nu = \left\{\frac{2}{\psi^2}\left[\pm \sqrt{\left(\frac{\varphi}{\psi} \pm \frac{1}{2\psi}\right)^2 - \frac{4}{\psi^2}\left[\frac{1}{16} - \frac{1}{\left(\frac{l}{t} c_f\right)^2_{hub}}\right]}\right]\right\}^{1/2} \tag{12}$$

Relation (12) was plotted in Fig. 14 with the hub ratio ν as ordinate, and $\frac{\varphi}{\psi}$, the quotient from two dimensionless quantities as abscissa and the pressure coefficient ψ as parameter.

The curves with continuous and with dashed lines refer to fans without and with prerotation, respectively. As seen, under otherwise identical conditions prerotation acts favourably on the relative hub dimensions.

On the basis of the theory expounded in Chapter 1, the prevention of eddy core emerges as a new requirement in the determination of the hub dimensions.

The conditions of eddy core formation in axial-flow fans, can best be followed by expressing the value of $\frac{Q}{\Gamma R}$ by the known dimensionless value $\frac{\varphi}{\psi}$ and the relative radius $\frac{r_i}{R}$. According to the above criteria, the numerator r_i, representing the radius of the eddy core, must be equal to the hub radius (R_b), since the denominator is the external fan radius, so the term $\frac{r_i}{R}$ is identical with the relative hub ratio applied in the preceding part.

And now, turning to the dimensionless quantities, the term $\frac{Q}{\Gamma R}$ may be written in the following form:

$$\frac{Q}{\Gamma R} = (1 - \nu^2) \frac{\varphi}{\psi} \tag{13}$$

Substituting Eq. (13) into the relation (9), we obtain

$$\frac{\varphi}{\psi} = \frac{\frac{1}{2}\sqrt{\frac{1}{2}\left(\frac{1}{\nu}\right)^2[1-\nu^2]^2 - [1-\nu^2]\ln\frac{1}{\nu}}}{1-\nu^2}\,. \tag{14}$$

Fig. 15 shows the dependence of the hub ratio on $\frac{\varphi}{\psi}$.

The curve indicates that the hub dimension needed to prevent the formation of eddy core decreases considerably with increasing $\frac{\varphi}{\psi}$ — regardless of the numerical values of φ and ψ.

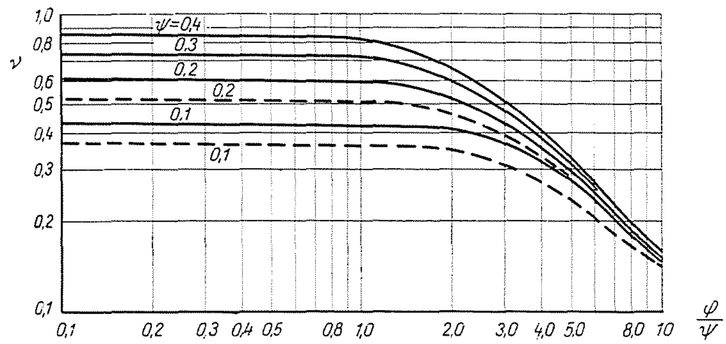

Fig. 14. Curves indicating the range of separation

According to the above it may be stated that the correct way to determine the dimensions of the hub of axial-flow fans is to take both restricting conditions simultaneously into consideration. Since in the restricting conditions the hub ratio had been represented by the same characteristics, so both curves can readily be illustrated in a common system. This, in turn, will make it possible to determine which of the curves will be the limiting one under the given conditions. Thus, in dimensioning, in possession of φ and ψ the correct hub ratio can be chosen without difficulty.

Fig. 16 is a common diagram of the curves of both limiting factors. It appears that for lower $\frac{\varphi}{\psi}$ values the condition to prevent an eddy core will determine the hub ratio, while for higher $\frac{\varphi}{\psi}$ values the condition to prevent separation will be determinant for the hub dimensions.

We have examined a number of different fans in use to check on the correctness of the dimensions of their hubs.

The characteristic $\frac{\varphi}{\psi}$ values were found to be within a range so that even the conventional process of hub design precluded eddy core formation.

This, however, does not mean that no special fans could, or would, be built with hubs dimensioned according to the new theory.

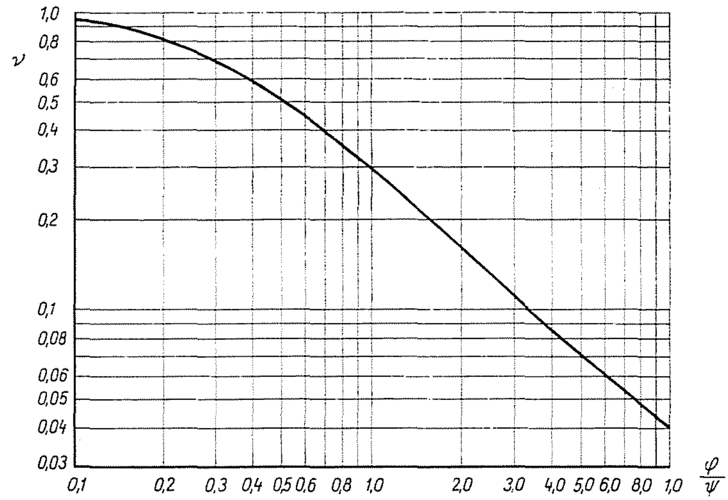

Fig. 15. Curve defining prevention of eddy core from forming

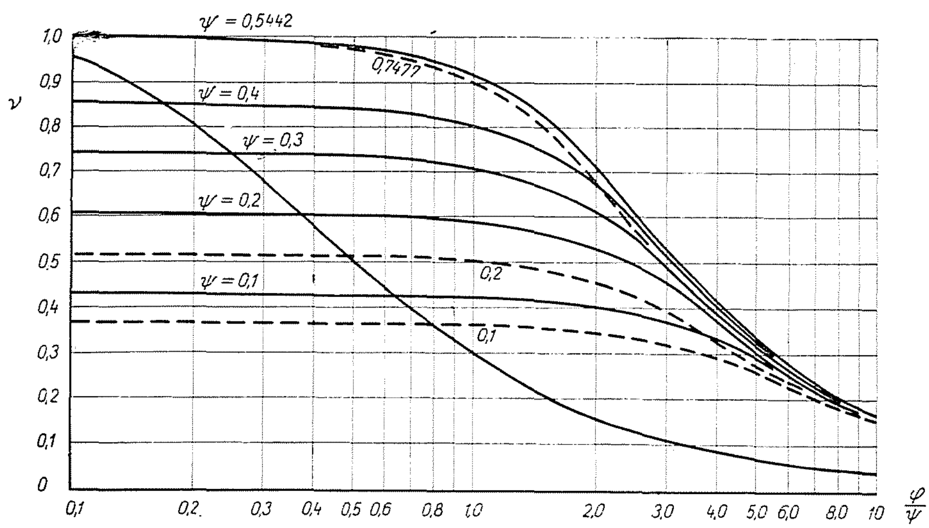

Fig. 16. Chart for the determination of the relative hub dimensions

The new phenomenon may have a particular significance in turbines where the pressure drop eliminates risk of separation and therefore the dimensions of the hub depend solely on the condition to prevent eddy cores from forming.

The problem is naturally far from being finally solved. Due to its novelty, it leaves many questions unanswered and calling for further investigation.

It would be useful, first of all, experimentally to determine the loss of efficiency due to eddy core formation and elucidate the effect on the eddy core of the compressibility of the medium.

Symbols

Q	rate of flow
Γ	spin
I	value of the effect integral
R	external radius
r_i	eddy core radius
R_b	hub radius
c	velocity of flow
c_a	axial velocity
c_u	meridional velocity
u	circumferential velocity of the impeller
w_1	relative inlet velocity
w_2	relative outlet velocity
w_∞	theoretical velocity of attack on the blade profile
c_1	absolute inlet velocity
c_2	absolute outlet velocity
Δc_u	circumferential velocity component determined by the blade circulation
ϱ	density of the flow medium
p_t	total pressure
Δp_t	increase of total pressure
p_0	environmental pressure
p_d	dynamic pressure
φ	flow coefficient
ψ	pressure coefficient
ν	relative hub dimensions
β_∞	angle included between w_∞ and u
δ	reciprocal gliding ratio

Subscripts

i	values for the parting surface radius
a	values for the hub radius
theor	theoretical or calculated values
k	physical characteristics for a radius R

Summary

During flow in cylindrical pipes with constant spin, an eddy core tends to form which does not take part in the mass transfer. In axial-flow machines the formation of an eddy core is undesirable and must be prevented by applying a hub of suitable dimensions. The diagrams presented in the paper are suitable for the direct determination of the hub ratio in axial-flow fans, with due consideration of all limiting factors.

References

1. Voith: Forschung und Konstruktion. Heft 5, (Oct. 1959).
2. GRUBER, J.: Ventilátorok (Fans), 1965. Műszaki Könyvkiadó, Budapest.

Dr. Ferenc BENCZE, Budapest XI., Bertalan Lajos u. 4—6. Hungary
László MOLNÁR, Budapest XI., Budafoki út 4. Hungary
Gábor DEMETER, Budapest XI., Fehérvári út 108/112. Hungary